Published in final edited form as:
Langmuir. 2017 March 21; 33(11): 2709–2716. doi:10.1021/acs.langmuir.6b04021.

Optimization of the Small Glycan Presentation for Binding a Tumor-Associated Antibody: Application to the Construction of an Ultrasensitive Glycan Biosensor

Filip Kveton[†], **Anna Blšáková**[†], **Andras Hushegyi**[†], **Pavel Damborsky**[†], **Ola Blixt**[‡], **Bo Jansson**[§], and **Jan Tkac**[*,†]

[†]Department of Glycobiotechnology, Institute of Chemistry, Slovak Academy of Sciences, Dubravska cesta 9, 845 38 Bratislava, Slovakia

[‡]Department of Chemistry, University of Copenhagen, 1871 Frederiksberg, Copenhagen, Denmark

[§]Division of Oncology and Pathology, Department of Clinical Sciences, Lund, Lund University, Lund, SE 221 85 Sweden

Abstract

The main aim of the study was to optimize the interfacial presentation of a small antigen - a Tn antigen (N-acetylgalactosamine) - for binding to its analyte anti-Tn antibody. Three different methods for the interfacial display of a small glycan are compared here, including two methods based on the immobilization of the Tn antigen on a mixed self-assembled monolayer (SAM) (2D biosensor) and the third one utilizing a layer of a human serum albumin (HSA) for the immobilization of a glycan forming a 3D interface. Results showed that the 3D interface with the immobilized Tn antigen is the most effective bioreceptive surface for binding its analyte. The 3D impedimetric glycan biosensor exhibited a limit of detection of 1.4 aM, a wide linear range (6 orders of magnitude), and high assay reproducibility with an average relative standard deviation of 4%. The buildup of an interface was optimized using various techniques with the visualization of the glycans on the biosensor surface by atomic force microscopy. The study showed that the 3D biosensor is not only the most sensitive compared to other two biosensor platforms but that the Tn antigen on the 3D biosensor surface is more accessible for antibody binding with better kinetics of binding ($t_{50\%}$ = 137 s, t50% = the time needed to attain 50% of a steady-state signal) compared to the 2D biosensor configuration with $t_{50\%}$ = 354 s. The 3D glycan biosensor was finally applied for the analysis of a human serum sample spiked with an analyte.

[*]**Corresponding Author**: Jan.Tkac@savba.sk. Tel: +421 2 5941 0263. Fax: +421 2 5941 0222.

ORCID
Ola Blixt: 0000-0003-4143-6276
Jan Tkac: 0000-0002-0765-7262

Notes
The authors declare no competing financial interest.

Europe PMC Funders Author Manuscripts

Europe PMC Funders Author Manuscripts

Introduction

Carbohydrates belong to four fundamental classes of biomolecules, along with proteins, nucleic acid, and lipids.1 Complex carbohydrates (glycans) are really important to a fundamental understanding of biology, and thanks to them we can develop new therapeutic and diagnostic strategies for major diseases.2 Glycans forming a large group of biomolecules with enormous structural complexity exist mainly in the form of glycoconjugates with proteins and lipids. Cell walls of all living cells are covered by glycans, which mediate the first contact in the host–pathogen interactions.3 Weak but highly specific protein–glycan interactions play important roles in many cellular processes, e.g., cell signaling, molecular recognition, immunity, tumor metastasis, leukocyte recruitment to sites of inflammation, and so forth.4

A large group of glycoconjugates is formed by the attachment of glycans to proteins via an asparagine residue (N-linked glycoproteins) or via serine/threonine (O-linked glycoproteins). 5 In recent years, the importance of changes in the glycan composition of O-linked glycans with the prominent role of the Tn antigen (i.e., N-acetylgalactosamine (GalNAc) linked to threonine or serine) in cancer development and progression was revealed with its presence in 70–90% of cancers.6 Moreover, the Tn antigen and its derivatives have a significant prognostic potential because their expression correlates well with the metastatic potential of cancer with a poor prognosis for cancers of the colon, lung, bladder, cervix, ovary, stomach, and prostate.6

Although the expression of the Tn antigen is without a doubt tumor-associated, the molecular mechanisms for its expression are still unclear but most likely linked to a lowered activity of glycosyltransferases or an increased activity of glycosidases.6,7 Thus, a direct detection of the Tn antigen attached to proteins circulating in the bloodstream might be an option for the detection of various types of cancer because this antigen is present in healthy individuals at a low level.6 The level of Tn antigen increases in an early stage of cancers (stage I and II patients) when it might be quite challenging to detect it. Because of an amplification of the antigenic signal by the immune system, autoantibodies against the Tn antigen and its derivatives could be detected in sera long before the Tn antigen.8 Thus, an analysis of autoantibodies against the Tn antigen using glycan arrays with immobilized Tn antigen and its derivatives can be utilized for the identification of an early stage of breast cancer with a prognostic potential.8 Moreover, the analysis of autoantibodies against the Tn antigen and its derivatives could be applied for assays of other types of cancer as well.6 Furthermore, the Tn-antigen-based vaccines can be applied to elicit an immune response with the production of antibodies against various types of cancer.9 An analysis of a panel of anti-Tn antibodies showed that whereas IgM antibodies preferentially bind to the terminal GalNAc residue, IgG antibodies recognize both the GalNAc epitope and a peptide sequence associated with GalNAc.10 Recent studies suggested that peptide sequences associated with the Tn antigen could affect also the binding of lectins with a K_D value that can be changed from 7 to 800 μM, indicating that lectin binding to short glycans also involves interactions with a peptide backbone.11–14 This is why it is worth investigating the immobilization of the Tn antigen on a peptide/protein backbone for the construction of the glycan biosensor.

Traditional glycan-printed arrays, although allowing extremely high throughput and flexible assays, are not particularly sensitive, with a typical concentration of protein analytes needed for the analysis of 1 nM.15 This is why alternative assay protocols able to provide analysis with an improved sensitivity of detection are sought.16 Because our recent work showed that impedimetric assays could be applied for an ultrasensitive analysis of a wide range of analytes,17,18 in this work we focused on the application of an impedimetric assay protocol for the analysis of the anti-Tn antibody with the glycan biosensor built with an immobilized Tn antigen. For this purpose, a gold electrode was applied; it can be easily patterned by thiols forming a SAM layer with the tunable density of functional groups19,20 applied for the immobilization of a glycan. SAMs can offer control of the density and orientation of immobilized glycan, which is beneficial to the investigation of a structure–activity relationship of multivalent interactions.21 Because the Tn antigen is small, i.e., formed by the attachment of one carbohydrate to one amino acid, in this study we optimized the way the Tn antigen is displayed on the biosensor interface. Three different strategies were compared: the immobilization of the Tn antigen either on two types of mixed SAMs (2D biosensor) or to an HSA protein attached to a mixed SAM layer (3D biosensor).

Materials and Methods

Chemicals

A complete list of abbreviations used for chemicals and instrumentation is in the Supporting Information file. Thiols HS−(CH2)3−EG2−OCH2−COOH [OEG−COOH, where EG = −(O−CH2−CH2)− and HS−(CH2)3−EG2−OH (OEG−OH)] were purchased from Prochimia (Poland). 11-Mercaptoundecanoic acid (MUA), 6-mercapto-1-hexanol (MH), potassium hexacyanoferrate(III), potassium hexacyanoferrate(II) trihydrate, potassium chloride, sodium hydroxide, sulfuric acid, N-hydroxysuccinimide (NHS), N-(3-(dimethylamino)propyl)-N′-ethylcarbodiimide hydrochloride (EDC), a phosphate-buffered saline tablet (PBS, one tablet dissolved in 200 mL of deionized water yields 0.01 M phosphate buffer, 0.0027 M potassium chloride, and 0.137 M sodium chloride, pH 7.4, at 25 °C), lectin from *Dolichos biflorus* (DBA), Concanavalin A (Con A), and human serum albumin (HSA) were purchased from Sigma-Aldrich (USA). Goat antimouse antibody (ab6708) applied as a nonspecific binding probe was purchased from Abcam (U.K.). Antibody GOD-2C4, a mouse IgG1κ antibody not cross-reacting with the GalNAc-β-O epitope or the blood group A antigen and specific to both synthetic Tn antigens and mucin-associated Tn antigen, was produced using a procedure published by Jansson and co-workers.22 Antibody GOD-2C4 binds to the Tn antigen expressed by cancer of the breast, colon, lung, ovary, and pancreas and was the first anti-Tn antibody showing antitumor activity on a solid tumor in vivo.22 Recently, the antibody was applied to identify a possible carrier of the Tn antigen in samples from patients having breast cancer.23 The binding specificity toward various glycans, glycoproteins, and proteins showed no binding of the GOD-2C4 antibody to BSA or HSA proteins with biospecific binding toward the Tn antigen.22 The Tn antigen (GalNAcα1-O-serine) was provided by Carbosynth (U.K.). Ethanol for UV/vis spectroscopy (ultrapure) was purchased from Slavus (Slovakia). All buffer components were dissolved in deionized water (DW). Proteins were dissolved in 10 mM PBS solution of pH 7.4 at a concentration of 1 mg mL^{-1} and were stored at −20 °C in aliquots.

Electrode Pretreatment and SAM Preparation

The cleaning of planar polycrystalline gold electrodes (d = 1.6 mm, Bioanalytical Systems, USA) was performed with an already-established protocol,24 with a laboratory potentiostat/galvanostat Autolab PGSTAT 128N (Ecochemie, Netherlands), in a three electrode cell with an Ag/AgCl reference and a counter Pt electrode (Bioanalytical Systems, USA). The first step was the reductive desorption of previously bound thiols in a 0.1 M solution of NaOH by applying a cyclic potential scanning from −1500 to −500 mV under an N2 atmosphere at a scan rate of 1 V s^{-1} for 50 cycles (until a stable scan was obtained). The second step was the mechanical polishing of the electrodes on a polishing pad using 1 μm particles for 5 min and 0.3 μm particles for 5 min (Buehler, USA). After mechanical polishing, the electrodes were sonicated two times in DW for 5 min. The third step was the immersion of the electrodes into a piranha solution (1:3 H_2O_2/H_2SO_4) for 20 min. (Caution! Handle piranha solution with special care because it is a strong oxidizing agent.) After piranha treatment, the electrodes were again sonicated in DW for 5 min. The fourth and fifth steps were electrochemical polishing and stripping in a 0.1 M solution of H_2SO_4. Electrochemical polishing was carried out by cyclic voltammetry, from −200 to 1500 mV at a scan rate of 100 mV s^{-1} for 25 cycles, and stripping was realized by 10 cycles starting from +750 to +200 mV at a scan rate of 100 mV s^{-1}. The electrodes were washed with DW and ultrapure ethanol. After the cleaning process, the electrodes were immersed in 1 mM solution of thiols) OEG−COOH/OEG−OH ratios of 1:1, 1:3, 1:5, and 1:10 or MUA/MH ratios of 1:3, 1:5, and 1:10) and incubated overnight in the dark at room temperature. The 1 mM stock solutions of thiols were prepared in ultrapure ethanol and stored at −20 °C.

Preparation of the Glycan Biosensors

After the incubation of the electrodes in the solution of thiols, they were washed with ultrapure ethanol and DW. Carboxyl groups on the SAM layer were activated with 40 μL of a solution of 200 mM EDC and 50 mM NHS in a ratio of 1:1 (solutions of EDC and NHS were previously prepared in DW and stored at −20 °C in aliquots) for 12 min. After activation, the electrodes were washed with DW and 100 μM Tn antigen was added to the biosensor surface (glycan was previously dissolved in 10 mM PBS pH 7.4 and stored at −20 °C in aliquots). The glycan immobilization was made at room temperature for 1.5 h. In case of a 3D glycan biosensor, after the activation of the −COOH group within a mixed SAM (OEG−COOH and OEG−OH) by EDC/NHS, the surface was incubated with HSA (10^{-4}–10^{-1} mg mL^{-1}) for 30 min. After the immobilization of HSA, the protein was activated with 40 μL of a solution of 200 mM EDC and 50 mM NHS in a ratio of 1:1 for 12 min, and then the activated surface was incubated with the Tn antigen (100 μM) for 1.5 h.

Electrochemical Impedance Spectroscopy (EIS) Measurements

EIS can provide the interfacial characteristics of a bioreceptive layer using a redox probe. The result of EIS analysis is presented in a Nyquist plot, from which such characteristics can be obtained. The method is sensitive to the thickness and density of biomolecules attached to the surface, resulting in a resistivity change of the biosensor surface.16,25 EIS was measured in an electrolyte containing 5 mM potassium hexacyanoferrate(III), 5 mM potassium hexacyanoferrate(II), and 0.01 M PBS at pH 7.4. The analysis was run at 50

different frequencies (ranging from 0.1 Hz up to 100 kHz) under Nova software 1.10 (Ecochemie, The Netherlands). The results were presented in the form of a Nyquist plot, with an equivalent circuit R(Q[RW]) applied for data fitting. The charge-transfer resistance (R_{CT}) parameter was used as the output signal for the calibration of the biosensor. Each analyte was measured at least in triplicate on three independent biosensor devices (electrodes), and the results are shown with a standard deviation (±SD) or relative standard deviation (RSD) calculated in Excel. It is worth noting that such RSDs are not relative standard errors of analyte detection but rather represent the reproducibility of the biosensor construction because each calibration curve was constructed by an independent biosensor device. Measurements of a particular analyte were performed on the same day.

Serum Sample Analysis

The human serum sample was collected from a control subject recruited from the Institute of Experimental Endocrinology, Slovak Academy of Sciences, Bratislava, Slovak Republic. The subject gave informed written consent, and the study was approved by the Ethics Committee of the National Institute for Rheumatic Diseases, Piestany, Slovak Republic, in accordance with the ethical guidelines of the Helsinki Declaration as revised in 2000. A blood sample was collected in a polyethylene tube with a clotting activator (S-Monovette, Sarstedt AG & Co., Germany). After centrifugation, the serum aliquot was stored at −80 °C until use. The serum sample was diluted in 10 mM PBS at pH 7.4 with a dilution ratio of 1:1000.

Quartz Crystal Microbalance (QCM) Measurements

QCM is a mechanical detection method used to measure the change in mass on a surface through the change in frequency of an oscillating quartz crystal. A decrease in the frequency of a QCM device is linearly proportional to the increased amount of species attached to the surface and can be applied to the calculation of the density of species present on the surface.[16,25] All QCM measurements were performed with Autolab PGSTAT 128N (Ecochemie, The Netherlands) equipment using an optional EQCM module. The changes in mass were evaluated using Sauerbrey's equation

$$\Delta f = -\frac{2f_0^2}{A\sqrt{\rho_q \mu_q}} * \Delta \mathrm{m} \quad (1)$$

, where Δf is the frequency change (Hz), f_0 is the nominal resonance frequency of the crystal (6 MHz), Δm is the change in mass (g cm^{-2}), μ_q is the shear modulus of quartz (g cm^{-1} s^{-2}), A is the surface area, and ρ_q is the density of quartz in g mL^{-1}. For a 6 MHz crystal, the whole equation can be simplified to

$$\Delta f = -C_f * m \quad (2),$$

where C_f is a frequency constant of 0.0815 Hz ng^{-1} cm^2. Assays were monitored and evaluated using the Nova 1.10 software, and all measurements were run at room temperature.

Surface Plasmon Resonance (SPR) Measurements

SPR is a frequently used optical detection method for following a binding event in real time, providing the kinetics of an interaction.16,25 Experiments were performed using a dual-channel Reichert SR7000DC SPR system controlled by SPR Autolink System software (AMETEK, Reichert Technologies, USA). For the SPR measurements, bare gold SPR sensor chips (XanTec Bioanalytics GmbH, Germany) were used. The bare gold SPR sensor chip was cleaned three times with piranha solution for 2–3 s and then washed with DW and ultrapure ethanol. Finally, the SPR chip was modified with thiols as described previously for the gold electrodes (Section 2.3).

The amount of Tn antigen immobilized on the surface of the 2D and 3D biosensors was investigated using the modified SPR sensor chip, i.e., OEG−OH/OEG−COOH SAM for the 2D biosensor and HSA immobilized on OEG−OH/OEG−COOH SAM for the 3D biosensor. The modified sensor chip was activated for 10 min (both working and reference channels of the SPR flow cell using a fresh mixture of 0.2 M EDC and 0.05 M NHS at a flow rate of 20 μL min^{-1}). Then, the Tn antigen (100 μM in 10 mM sodium acetate buffer at pH 4.5) was injected into the working channel for 48 min (an association phase). At the end of the SPR experiment, a dissociation phase was induced by the injection of 0.01 M PBS for 20 min at a flow rate of 20 μL min^{-1}. Finally, the SPR response in the working channel was subtracted from the SPR signal read in the reference channel. For the calculation of the total amount of bound Tn antigen, the conversion 1 mRIU = 1 pg mm^{-2} (according to the manufacturer) was applied.

Atomic Force Microscopy (AFM) Measurements

AFM is applied to visualize interfacial features at the nanoscale.17 For AFM visualization, a Bioscope Catalyst instrument and an Olympus IX71 microscope in conjunction with NanoScope 8.15 software were run at a scan rate of 0.5 line s^{-1} with the tip set to 200 pN (Scan Asyst, Bruker, USA). Measurements were made using peak force tapping mode in air. Bare gold SPR sensor chips (XanTec Bioanalytics GmbH, Germany) were cleaned three times with piranha solution for 2–3 s and then with DW and ultrapure ethanol, and the chips were modified with thiols and glycans, as described previously. The SCANASYSTAIR silicon tip on a nitride lever (Bruker, USA, with f 0 = 50–90 kHz and k = 0.4 N m^{-1}), sharpened to a tip radius of 2 nm, was used in the assays.

Results and Discussion

Glycan Biosensor Based on the MUA/MH SAM (Biosensor 1)

In the previous study, we prepared an ultrasensitive glycan biosensor based on a mixed SAM composed of MUA and MH with immobilized sialyllactose for the detection of glycan binding proteins.17 Here we wanted to test the same interfacial SAM for the immobilization of the Tn antigen for the subsequent detection of an anti-Tn antibody (GOD-2C4) and DBA

lectin. The results showed that the optimal composition of a mixed SAM for the construction of the Tn biosensor contains 16.7% MUA in the mixture (Figure 1 and Figure S1). Taking into an account the distance between neighboring thiols of 0.5 nm,20 an average distance between neighboring MUA thiols in a mixed SAM composed of 16.7% MUA would be 1.4 nm. The length difference between MUA (~1.7 nm) and MH (~1.1 nm) of 0.6 nm might be sufficient to partially accommodate the Tn antigen (~1.0 nm × 1.0 nm) within a mixed SAM composed of MUA and MH (Figure 2A), which would negatively influence the binding performance between glycan and the antibody. An examination of the selectivity of the glycan biosensor showed that the sensitivity of detection of GOD-2C4 was (8.3 ± 1.0)% decade^{-1} (R^2 = 0.961) in the concentration window of 14 aM–14 fM with an average RSDof assays of 18% (12–23%). The biosensor sensitivity for DBA of (4.4 ± 0.2)% decade^{-1} (R2 = 0.991) and HSA of (4.4 ± 0.1)% decade^{-1} (R^2 = 0.994) was similar to the drift in the biosensor signal, when incubated in PBS buffer, so it can be concluded that DBA and HSA did not interact with the glycan biosensor.

Glycan Biosensor Based on the OEG−COOH/OEG−OH SAM (Biosensor 2)

Optimization experiments showed that the optimal SAM for the construction of the glycan biosensor should contain 25% OEG−COOH thiol in a mixture (Figure S2), but the glycan biosensor built on such a mixed SAM exhibited a rather high average RSD of assays of 39%, whereas the glycan biosensor built on a mixed SAM containing 16.7% OEG−COOH exhibited an average RSD of assays of 18% (1–28%). The glycan biosensor constructed on a SAM containing 16.7% OEG−COOH could detect GOD-2C4 with a sensitivity of (4.7 ± 0.5)% decade^{-1} (R^2 = 0.938), a limit of detection (LOD) of 110 aM, and a linear concentration range from 110 aM to 140 pM (~6 orders of magnitude). Moreover, DBA could be effectively detected with this glycan biosensor with a sensitivity of (6.2 ± 0.3)% decade^{-1} (R^2 = 0.987), a LOD of 270 aM, and a linear concentration range from 270 aM to 140 pM (~6 orders of magnitude). It is interesting that for DBA lectin the Tn antigen exposed on the SAM composed of OEG−COOH and OEG−OH is accessible for binding, most likely because the Tn antigen cannot be easily buried within this SAM layer (Figure 2B) compared to a previous case (MUA/MH SAM, Figure 2A). DBA binding is more effective compared to GOD-2C4 binding to the immobilized Tn antigen with a sensitivity ratio of 1.3 (= 6.2/4.7).

Most importantly the glycan biosensor is not sensitive toward nonselective binding probe HSA, and no signal drift was observed when the glycan biosensor was incubated with PBS (Figure 3 and Figure S2), making the glycan biosensor stable and selective.

Glycan Biosensor Based on HSA Attached to the OEG−COOH/OEG−OH SAM (Biosensor 3)

The third type of interfacial layer tested as a support to accommodate the Tn antigen was a layer of HSA protein covalently attached to OEG−COOH/OEG−OH SAM (1:5 OEG −COOH/OEG−OH). Four different HSA concentrations were applied for HAS immobilization, i.e., 0.0001, 0.001, 0.01, and 0.1 mg mL^{-1}, with the highest sensitivity of the glycan biosensor achieved with the one built on the HSA layer deposited from 0.001 mg mL^{-1} HSA solution (Figure S3). The glycan biosensor constructed with an optimal HSA composition could detect both analytes: GOD-2C4 and DBA (Figure 4). The antibody could

be detected with a sensitivity of (6.7 ± 0.1)% decade^{-1} (R^2 = 0.998), a LOD of 1.4 aM, and a linear concentration range from 1.4 aM to 1.4 pM (~6 orders of magnitude). Moreover, the assay reproducibility was very high, with an average RSD of 4% (1−9%). DBA could be detected with a sensitivity of (9.3 ± 0.3)% decade^{-1} (R^2 = 0.994), a LOD of 36 aM, and a linear concentration range from 36 aM to 1.4 pM (~5 orders of magnitude). Again, DBA binding is more effective compared to GOD-2C4 binding to the immobilized Tn antigen with a sensitivity ratio of 1.4 (= 9.3/6.8). This value is very similar to the value of 1.3 obtained with glycan biosensor 2 based on the OEG-COOH/OEG−OH SAM layer without an HSA layer present.

The selectivity of the biosensor was tested using HSA as a nonselective binding probe (Figure 4), lectin Concanavalin A, and goat antimouse antibody not recognizing the Tn antigen (Figure S4), showing only minor binding.

SPR Experiments for the Calculation of the Immobilized Tn Antigen (Biosensor 2 vs Biosensor 3)

SPR experiments revealed that the Tn antigen after the covalent attachment to the biosensor 2 surface gave a response of 140 μRIU, equivalent to a surface density of 140 pg mm^{-2} (46 pmol cm^{-2}). If we take into account that the Tn antigen has a projected surface area of ~1 nm^2, then a theoretical surface coverage for the surface-confined Tn antigen would be 170 pmol cm^{-2}, indicating that the Tn antigen on the interface of biosensor 2 occupies 27% of the theoretical coverage.

In case of biosensor 3 (i.e., 3D configuration), the SPR response after the covalent attachment of the Tn antigen was 870 μRIU, equivalent to a surface density of 870 pg mm^{-2} (290 pmol cm^{-2}). The surface of glycan biosensor 3 built on molecular HSA scaffolds will have a larger (~2-fold) surface area due to HSA molecules present compared to the surface without this protein layer. Thus, it can be anticipated that a theoretical surface coverage for the Tn antigen on the HAS layer would be 340 pmol cm^{-2} (per geometric surface area), indicating that the Tn antigen on the interface of biosensor 3 occupies 85% of the theoretical coverage.

When only a geometric surface area is taken into account, a 6.3-fold-higher surface density of the Tn antigen on the interface of biosensor 3 was immobilized compared to the interface of biosensor 2.

QCM Experiments: Biosensor 2 vs Biosensor 3

QCM experiments were run to understand what amount of analyte, GOD-2C4, can be attached to the Tn-antigen-modified interfaces of biosensors 2 and 3. Results showed that after the injection of GOD-2C4 at a concentration of 3.3 nM a change in the frequency of the QCM crystal of −15.7 Hz (193 ng cm^{-2} or 1.3 pmol cm^{-2}, i.e., 51% of a theoretical full monolayer) was observed on the surface of biosensor 2 (Figure S5). A slightly larger QCM response of −22.0 Hz (270 ng cm^{-2} or 1.8 pmol cm^{-2}, i.e., 36% of a theoretical full monolayer) was observed on the interface of biosensor 3 (Figure S5). When only a geometric surface area is taken into account, then the amount of GOD-2C4 analyte attached to the biosensor 3 interface is 1.4-fold higher compared to that of biosensor 2. Results from

EIS measurements confirmed that the sensitivity of GOD-2C4 detection is 1.4-fold higher on biosensor 3 than on biosensor 2. Thus, results obtained by QCM and EIS, two independent assay methods, are in an excellent agreement.

It is quite interesting to directly compare the kinetics of GOD-2C4 analyte binding to the Tn antigen present on the OEG−COOH/OEG−OH SAM layer (biosensor 2) or to the Tn antigen present on a monolayer of HSA protein (biosensor 3) (Figure S6). Results from such an experiment showed that the binding of GOD-2C4 is quicker ($t_{50\%}$ = 137 s) on biosensor 3 compared to the response on biosensor 2 with $t_{50\%}$ = 354 s (Figure S6). This confirms the better accessibility of the Tn antigen on the HSA layer compared to the interface without an immobilized HSA layer.

AFM Experiments: Biosensor 2 vs Biosensor 3

A closer look at the modified biosensor surfaces visualized by AFM revealed that glycan biosensor 2 with the Tn antigen immobilized on a mixed OEG-COOH/OEG−OH SAM layer exhibits a rougher interface (Figures 5A and 6A) as a result of the natural roughness of the gold layer compared to the roughness of an interfacial layer of biosensor 3 with the Tn antigen present on an HSA layer (Figures 5C and 6B). An analysis of the profile of features present on both types of biosensors (Figure 6) confirms the fact that biosensor 2 interface before interaction with the GOD-2C4 analyte is rougher (R_q = 0.32 nm) compared to the interface of biosensor 3 (R_q = 0.09 nm) (Figure 6). After the incubation of the GOD-2C4 analyte with both biosensor surfaces, it was possible to see individual antibody molecules attached to the Tn antigen (Figure 5B,D). The roughness of the biosensor 2 interface increased from R_q = 0.32 to 1.8 nm after incubation with an analyte, and the roughness of the surface of biosensor 3 increased from R_q = 0.09 to 0.89 nm. Quite high roughness of the interface of biosensor 2 before interaction with the bound GOD-2C4 analyte having features with a height of ±2 nm might cause the Tn antigen to be less available for binding to GOD-2C4 compared to the situation on the surface of biosensor 3 with the height of features before the incubation of GOD-2C4 of only ±0.2 nm. Thus, the HSA layer can suppress the natural nanoscale roughness of the gold film, which is a feature important for the effective display of short glycans such as the Tn antigen with a size of ~(1.0 × 1.0) nm for subsequent protein binding.

When we looked at the structure of the HSA molecule, we found that HSA has at least 10 acidic amino acids available for further activation by EDC/NHS, of which 6 are glutamic acids (Glu132, Glu266, Glu280, Glu479, Glu492, and Glu501) and 4 are aspartic acids (Asp269, Asp301, Asp471, and Asp562) (Figure S7), and thus quite a few glycans can be attached to one HSA molecule.

Comparison of the Glycan Biosensors with Published Concepts

Recently, a comparison study with the involvement of six different platforms for the construction of glycan arrays applied to the detection of four lectins was performed. The results clearly showed that a microarray with short glycans (GalNAc and other monosaccharide determinants) attached to proteins (bovine serum albumin (BSA) or HSA) exhibited a response after incubation with lectins, whereas the response on a glycan

microarray with glycans directly printed on the microscope slide did not reveal any binding.15 This confirms that short glycans/carbohydrate antigens have to be displayed so as to be accessible for binding, which could be achieved by the presentation of glycans on the backbone of a protein. The importance of the Tn antigen presentation on a peptide backbone for effective binding of anti Tn-antibodies was discussed in a recent review as well.26 Moreover, glycans attached to the backbone of the BSA/HSA protein can be displayed at similar densities as present on natural glycoproteins, 27,28 a feature important for getting physiologically relevant information.

Classical ELISA with a glycan immobilized on a BSA backbone showed an LOD of 140 nM, whereas the immobilization of a glycan on gold nanoparticles with a size of 2 nm showed an LOD of 50 pM for the analysis of IgGs.29 Using the glycan array constructed with the dendrons, the LOD for antibody detection was 350 pM,30 and a LOD of 4 nM for the determination of antibodies was achieved in the conventional ELISA plates.31 In another paper, three different analytical platforms based on immobilized glycans for the detection of antibodies were compared, and although the LOD was not quantified, a linear calibration curve started from 10, 250, and 700 pM for an ELISA-like format, for a suspension-based array and for a typical glycan microarray, respectively.32 When the biosensor platforms (SPR, localized SPR, QCM, field-effect sensing FET, various electrochemical approaches, and cantilever-based assays) of detection are taken into account, a typical LOD for the detection of various analytes with the glycan biosensors is down to the nanomolar to picomolar range.16 The only exception was the FET sensing of influenza hemagglutinins with a LOD down to attomolar level.33 Recently, we showed that lectins could be detected down to concentration of 8 aM17,18 and hemagglutinins down to a concentration of 140 aM.17 This means that the glycan biosensor based on the Tn antigen immobilized on the HAS layer not only is the most sensitive Tn-glycan-based device for lectin detection with a LOD of 36 aM and for antibody detection with a LOD of 1.4 aM but also belongs to the most sensitive electrical biosensors for the detection of disease biomarkers described so far.1,34 High sensitivity of the detection by the glycan biosensor could be important in cases in which the density of the Tn antigen in the human body is high, with Tn antibodies mainly bound to such antigens, resulting in a low circulating concentration of Tn antibodies.

Analysis of a Spiked Serum Sample

A serum sample from a healthy individual was spiked with three different concentrations of GOD-2C4 antibody (0.1, 1, and 10 pM), and such analysis revealed a sensitivity for GOD-2C4 antibody detection of 6.0% decade^{-1}, which is slightly lower compared to a sensitivity of detection of the same analyte in a plain buffer of 6.7% decade^{-1}, i.e., 90% of the biosensor sensitivity obtained in buffer equal to a recovery index of 90%. This can be ascribed to the matrix effect of a complex human serum sample as described in numerous studies, when recovery indexes of 55%,35 67%,36 74%,37 91%,38 and 97%39 were determined for various analytes and dilutions. Thus, the recovery index of 90% is within the range previously published by others. Obviously, an analysis of more samples would be needed in the future to make more general conclusions about the performance of the glycan biosensor in the analysis of real samples. There are numerous possible applications of the Tn-based glycan biosensor, which can be applied for the detection of (A) autoantibodies to

the Tn antigen present in serum during cancer development and progression;8 (B) antibodies against the Tn antigen injected into humans during passive immunotherapy;22 (C) antibodies elicited against the Tn antigen after treatment by the Tn antigen-based vaccines during active immunization of cancer patients;8,9 (D) anti-Tn antibodies present in the supernatant from hybridomas cultures during their production;22 and (E) the analysis of a refolding efficiency during the production of antibody fragments against the Tn antigen by a recombinant technology.40 There is, however, a need to employ impedimetric assays into an array format of analysis with a minor degree of multiplexing, which is a feasible task, as shown for lectin biosensors recently by us using a chip with eight electrodes.41 Furthermore, efficient approaches designed by Davis' laboratory regarding how to deal with the matrix effect of serum could be applied to the construction of glycan biosensors as well. Additionally, the effect of a peptide environment close to the immobilized Tn antigen on the biosensor performance should be tested in the future as well.42–44

Conclusions

The study showed that the best way to present a small glycan such as the Tn antigen for subsequent binding of the anti Tn-antibody is the immobilization of the glycan on the HSA layer. This study strongly supports conclusions made by a comparative study of the requirement to present small glycans on a protein backbone to make glycans accessible to their binders. Moreover, the glycan biosensor based on the HAS layer (3D biosensor) offered much better analytical performance than the glycan biosensor based on the 2D configuration in terms of sensitivity (6.7 vs 4.7% decade^{-1}), linear range (1.4 aM–1.4 pM with R^2 = 0.998 vs. 270 aM–1.4 pM with R^2 = 0.987), LOD (1.4 vs. 270 aM), average RSD (4 vs. 18%), and kinetics of interactions ($t_{50\%}$ = 137 s vs. $t_{50\%}$ = 354 s). Moreover, the 3D biosensor exhibits a much lower surface roughness of 0.09 nm compared to the value of 0.32 nm observed for the 2D biosensor configuration. This is an important issue for the proper interfacial display of a small glycan such as the Tn antigen and also for the surface presentation of other small ligands, which is not an issue for the detection of auto antibodies produced against protein targets.42–44

Supplementary Material

Refer to Web version on PubMed Central for supplementary material.

Acknowledgments

This publication was made possible by NPRP grant no. 6-381-1-078 from the Qatar National Research Fund (a member of the Qatar Foundation). The statements made herein are solely the responsibility of the authors. Funding from the Slovak Research and Development Agency (APVV-14-0753 and VEGA 2/0162/14) is acknowledged. The research leading to these results has received funding from the European Research Council under the European Union's Seventh Framework Program [(FP/2007-2013)/ERC grant agreement no. 311532]. This publication is the result of the project implementation (Centre for Materials, Layers and Systems for Applications and Chemical Processes under Extreme Conditions, stage I, ITMS no. 26240120007) supported by the Research & Development Operational Program funded by the ERDF.

References

(1). Paleček E, Tkáč J, Bartošík M, Bertók T, Ostatná V, Paleček J. Electrochemistry of non-conjugated proteins and glycoproteins. Towards sensors for biomedicine and glycomics. Chem Rev. 2015; 115:2045–2108. [PubMed: 25659975]

(2). Dalziel M, Crispin M, Scanlan CN, Zitzmann N, Dwek RA. Emerging principles for the therapeutic exploitation of glycosylation. Science. 2014; 343:1235681. [PubMed: 24385630]

(3). Rouvinski A, Guardado-Calvo P, Barba-Spaeth G, Duquerroy S, Vaney MC, Kikuti CM, Navarro Sanchez ME, Dejnirattisai W, Wongwiwat W, Haouz A, Girard-Blanc C, et al. Recognition determinants of broadly neutralizing human antibodies against dengue viruses. Nature. 2015; 520:109–13. [PubMed: 25581790]

(4). Reichardt NC, Martín-Lomas M, Penadés S. Glyconanotechnology. Chem Soc Rev. 2013; 42:4358–4376. [PubMed: 23303404]

(5). Park S, Gildersleeve JC, Blixt O, Shin I. Carbohydrate microarrays. Chem Soc Rev. 2013; 42:4310–4326. [PubMed: 23192235]

(6). Ju T, Otto VI, Cummings RD. The Tn Antigen-Structural Simplicity and Biological Complexity. Angew Chem, Int Ed. 2011; 50:1770–1791.

(7). Ju T, Aryal RP, Kudelka MR, Wang Y, Cummings RD. The Cosmc connection to the Tn antigen in cancer. Cancer Biomarkers. 2014; 14:63–81. [PubMed: 24643043]

(8). Blixt O, Bueti D, Burford B, Allen D, Julien S, Hollingsworth M, Gammerman A, Fentiman I, Taylor-Papadimitriou J, Burchell JM. Autoantibodies to aberrantly glycosylated MUC1 in early stage breast cancer are associated with a better prognosis. Breast Cancer Res. 2011; 13:1.

(9). Marchetti R, Perez S, Arda A, Imberty A, Jimenez-Barbero J, Silipo A, Molinaro A. Rules of Engagement" of Protein–Glycoconjugate Interactions: A Molecular View Achievable by using NMR Spectroscopy and Molecular Modeling. ChemistryOpen. 2016; 5:274. [PubMed: 27547635]

(10). Blixt O, Lavrova OI, Mazurov DV, Cló E, Kračun SK, Bovin NV, Filatov AV. Analysis of Tn antigenicity with a panel of new IgM and IgG1 monoclonal antibodies raised against leukemic cells. Glycobiology. 2012; 22:529–542. [PubMed: 22143985]

(11). Madariaga D, Martínez-Sáez N, Somovilla VJ, Coelho H, Valero-González J, Castro-López J, Asensio JL, Jiménez-Barbero Js, Busto JsH, Avenoza A. Detection of tumor-associated glycopeptides by lectins: The peptide context modulates carbohydrate recognition. ACS Chem Biol. 2015; 10:747–756. [PubMed: 25457745]

(12). Martínez-Sáez N, Castro-López J, Valero-González J, Madariaga D, Compañón I, Somovilla VJ, Salvadó M, Asensio JL, Jiménez-Barbero J, Avenoza A. Deciphering the Non-Equivalence of Serine and Threonine O-Glycosylation Points: Implications for Molecular Recognition of the Tn Antigen by an anti-MUC1 Antibody. Angew Chem Int Ed. 2015; 54:9830–9834.

(13). Sterner E, Flanagan N, Gildersleeve JC. Perspectives on Anti-Glycan Antibodies Gleaned from Development of a Community Resource Database. ACS Chem Biol. 2016; 11:1773–83. [PubMed: 27220698]

(14). Borgert A, Heimburg-Molinaro J, Song X, Lasanajak Y, Ju T, Liu M, Thompson P, Ragupathi G, Barany G, Smith DF. Deciphering structural elements of mucin glycoprotein recognition. ACS Chem Biol. 2012; 7:1031–1039. [PubMed: 22444368]

(15). Wang L, Cummings RD, Smith DF, Huflejt M, Campbell CT, Gildersleeve JC, Gerlach JQ, Kilcoyne M, Joshi L, Serna S, Reichardt NC. Cross-platform comparison of glycan microarray formats. Glycobiology. 2014; 24:507–17. [PubMed: 24658466]

(16). Hushegyi A, Tkac J. Are glycan biosensors an alternative to glycan microarrays? Anal Methods. 2014; 6:6610–6620. [PubMed: 27231487]

(17). Hushegyi A, Bertok T, Damborsky P, Katrlik J, Tkac J. An ultrasensitive impedimetric glycan biosensor with controlled glycan density for detection of lectins and influenza hemagglutinins. Chem Commun. 2015; 51:7474–7477.

(18). Hushegyi A, Pihíková D, Bertok T, Adam V, Kizek R, Tkac J. Ultrasensitive detection of influenza viruses with a glycan-based impedimetric biosensor. Biosens Bioelectron. 2016; 79:644–649. [PubMed: 26765527]

(19). Lahiri J, Isaacs L, Tien J, Whitesides GM. A Strategy for the Generation of Surfaces Presenting Ligands for Studies of Binding Based on an Active Ester as a Common Reactive Intermediate: A Surface Plasmon Resonance Study. Anal Chem. 1999; 71:777–790. [PubMed: 10051846]

(20). Love JC, Estroff LA, Kriebel JK, Nuzzo RG, Whitesides GM. Self-assembled monolayers of thiolates on metals as a form of nanotechnology. Chem Rev. 2005; 105:1103–1170. [PubMed: 15826011]

(21). Yang J, Chazalviel J-N, Siriwardena A, Boukherroub R, Ozanam F, Szunerits S, Gouget-Laemmel AC. Quantitative Assessment of the Multivalent Protein–Carbohydrate Interactions on Silicon. Anal Chem. 2014; 86:10340–10349. [PubMed: 25216376]

(22). Welinder C, Baldetorp B, Borrebaeck C, Fredlund B-M, Jansson B. A new murine IgG1 anti-Tn monoclonal antibody with in vivo anti-tumor activity. Glycobiology. 2011; 21:1097–1107. [PubMed: 21470982]

(23). Welinder C, Baldetorp B, Blixt O, Grabau D, Jansson B. Primary breast cancer tumours contain high amounts of IgA1 immunoglobulin: an immunohistochemical analysis of a possible carrier of the tumour-associated Tn antigen. PLoS One. 2013; 8:e61749. [PubMed: 23637900]

(24). Tkac J, Davis JJ. An optimized electrode pre-treatment for SAM formation on polycrystalline gold. J Electroanal Chem. 2008; 621:117–120.

(25). Klukova L, Bertok T, Kasák P, Tkac J. Nanoscale-controlled architecture for the development of ultrasensitive lectin biosensors applicable in glycomics. Anal Methods. 2014; 6:4922–4931. [PubMed: 27231486]

(26). Fujita-Yamaguchi Y. Production of single-chain variable-fragments against carbohydrate antigens. Antibodies. 2014; 3:155–168.

(27). Muthana SM, Gildersleeve JC. Factors Affecting Anti-Glycan IgG and IgM Repertoires in Human Serum. Sci Rep. 2016; 6:19509. [PubMed: 26781493]

(28). Muthana SM, Xia L, Campbell CT, Zhang Y, Gildersleeve JC. Competition between serum IgG, IgM, and IgA anti-glycan antibodies. PLoS One. 2015; 10:e0119298. [PubMed: 25807519]

(29). Chiodo F, Marradi M, Tefsen B, Snippe H, van Die I, Penadés S. High sensitive detection of carbohydrate binding proteins in an ELISA-solid phase assay based on multivalent glyconanoparticles. PLoS One. 2013; 8:e73027. [PubMed: 24014084]

(30). Wang S-K, Liang P-H, Astronomo RD, Hsu T-L, Hsieh S-L, Burton DR, Wong C-H. Targeting the carbohydrates on HIV-1: Interaction of oligomannose dendrons with human monoclonal antibody 2G12 and DC-SIGN. Proc Natl Acad Sci USA. 2008; 105:3690–3695. [PubMed: 18310320]

(31). Astronomo RD, Kaltgrad E, Udit AK, Wang S-K, Doores KJ, Huang C-Y, Pantophlet R, Paulson JC, Wong C-H, Finn M. Defining criteria for oligomannose immunogens for HIV using icosahedral virus capsid scaffolds. Chem Biol. 2010; 17:357–370. [PubMed: 20416507]

(32). Pochechueva T, Jacob F, Goldstein DR, Huflejt ME, Chinarev A, Caduff R, Fink D, Hacker N, Bovin NV, Heinzelmann-Schwarz V. Comparison of printed glycan array, suspension array and ELISA in the detection of human anti-glycan antibodies. Glycoconjugate J. 2011; 28:507–517.

(33). Hideshima S, Hinou H, Ebihara D, Sato R, Kuroiwa S, Nakanishi T, Nishimura S-I, Osaka T. Attomolar detection of influenza A virus hemagglutinin human H1 and avian H5 using glycan-blotted field effect transistor biosensor. Anal Chem. 2013; 85:5641–5644. [PubMed: 23675869]

(34). Luo X, Davis JJ. Electrical biosensors and the label free detection of protein disease biomarkers. Chem Soc Rev. 2013; 42:5944–5962. [PubMed: 23615920]

(35). Gamella M, Campuzano S, Conzuelo F, Reviejo AJ, Pingarrón JM. Amperometric Magnetoimmunosensors for Direct Determination of D-Dimer in Human Serum. Electroanalysis. 2012; 24:2235–2243.

(36). Xu M, Luo X, Davis JJ. The label free picomolar detection of insulin in blood serum. Biosens Bioelectron. 2013; 39:21–25. [PubMed: 22840329]

(37). Cecchetto J, Carvalho FC, Santos A, Fernandes FC, Bueno PR. An impedimetric biosensor to test neat serum for dengue diagnosis. Sens Actuators B. 2015; 213:150–154.

(38). de Ávila BEF, Escamilla-Gómez V, Campuzano S, Pedrero M, Pingarrón JM. Disposable electrochemical magnetoimmunosensor for the determination of troponin T cardiac marker. Electroanalysis. 2013; 25:51–58.

(39). Bryan T, Luo X, Bueno PR, Davis JJ. An optimized electrochemical biosensor for the label-free detection of C-reactive protein in blood. Biosens Bioelectron. 2013; 39:94–98. [PubMed: 22809521]

(40). Arakawa T, Ejima D. Refolding Technologies for Antibody Fragments. Antibodies. 2014; 3:232–241.

(41). Bertok T, Dosekova E, Belicky S, Holazova A, Lorencova L, Mislovicova D, Paprckova D, Vikartovska A, Plicka R, Krejci J. Mixed Zwitterion-Based Self-Assembled Monolayer Interface for Impedimetric Glycomic Analyses of Human IgG Samples in an Array Format. Langmuir. 2016; 32:7070–7078. [PubMed: 27311591]

(42). Bryan T, Luo X, Forsgren L, Morozova-Roche LA, Davis JJ. The robust electrochemical detection of a Parkinson's disease marker in whole blood sera. Chem Sci. 2012; 3:3468–3473.

(43). Xu Q, Cheng H, Lehr J, Patil AV, Davis JJ. Graphene Oxide Interfaces in Serum Based Autoantibody Quantification. Anal Chem. 2015; 87:346–350. [PubMed: 25514013]

(44). Xu Q, Evetts S, Hu M, Talbot K, Wade-Martins R, Davis JJ. An impedimetric assay of α-synuclein autoantibodies in early stage Parkinson's disease. RSC Adv. 2014; 4:58773–58777.

Europe PMC Funders Author Manuscripts

Europe PMC Funders Author Manuscripts

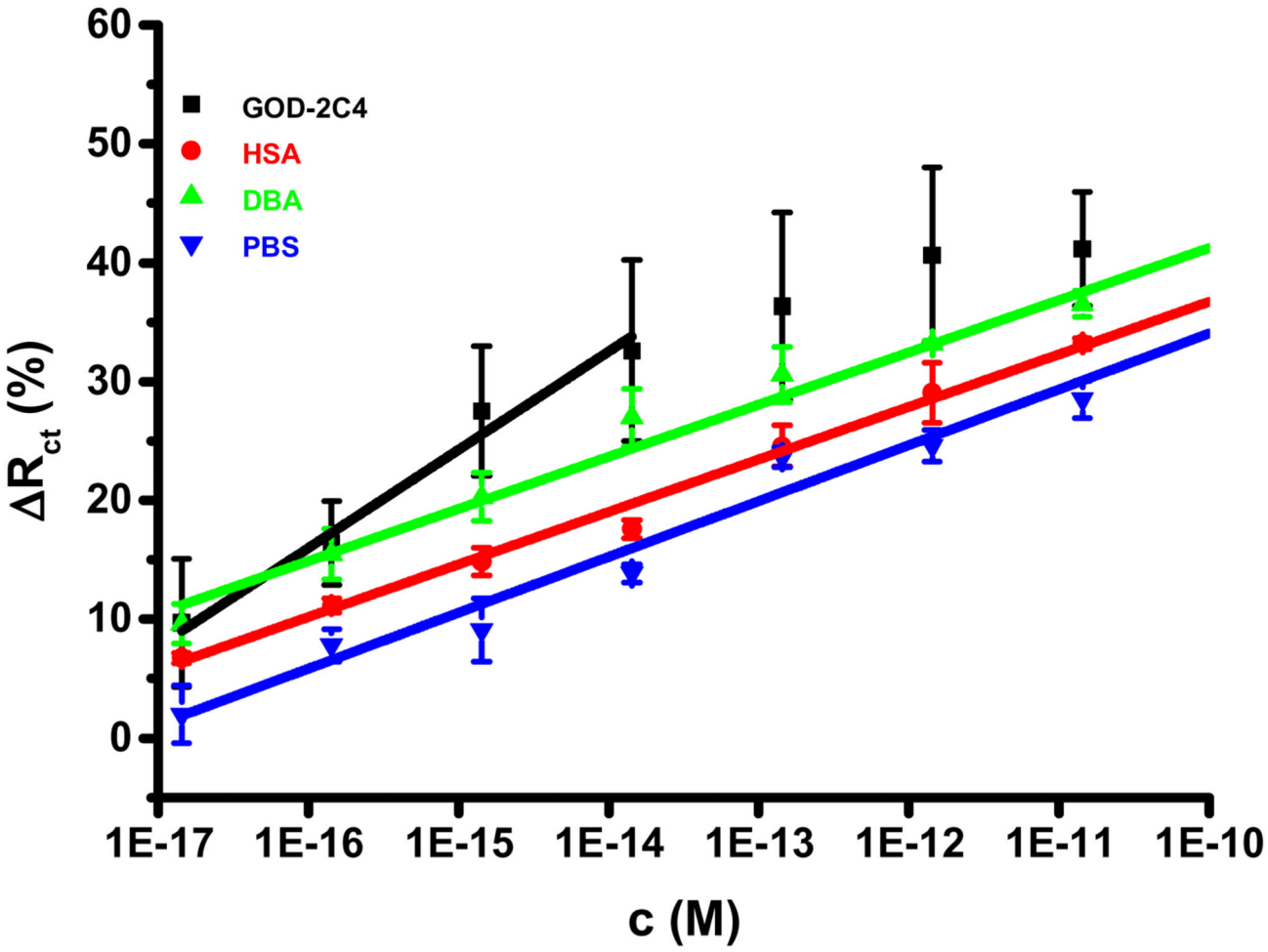

Figure 1.

Selectivity of the glycan biosensor constructed on a mixed SAM containing 16.7% of MUA in a thiol mixture was probed by analysis of two analytes (GOD-2C4 and DBA) and a non-specific binding probe (HSA). Moreover, a drift of the signal of the biosensor incubated only with PBS measured at the same time intervals as for GOD-2C4, HSA and DBA is shown, as well. At least three independent electrodes were used for data generation. EIS assays were performed in an electrolyte containing 5 mM potassium hexacyanoferrate (III), 5 mM potassium hexacyanoferrate (II) and 0.01 M PBS, pH 7.4. The analysis was run at 50 different frequencies (0.1 Hz - 100 kHz) at room temperature.

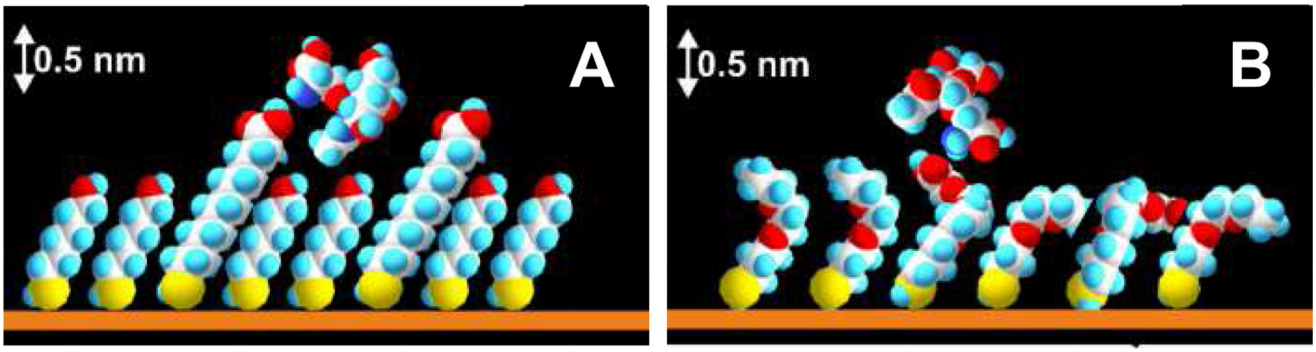

Figure 2.

A mixed SAM composed of MUA and MH attached to gold with the Tn antigen shown above a mixed SAM layer (**A**) and a mixed SAM composed of OEG-COOH and OEG-OH with the Tn antigen shown above a mixed SAM layer, as well (**B**). Both figures are drawn to scale.

Europe PMC Funders Author Manuscripts

Europe PMC Funders Author Manuscripts

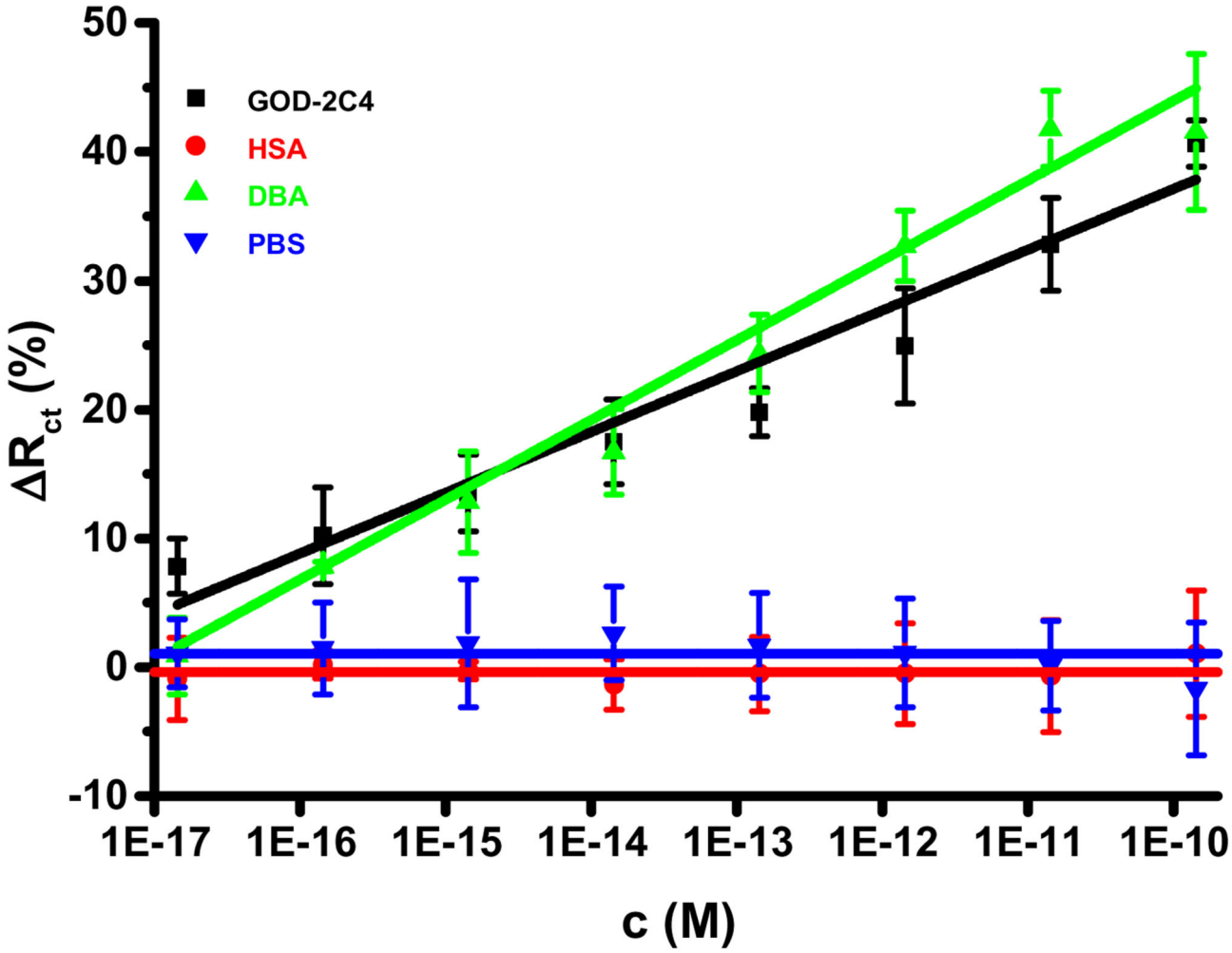

Figure 3.

Selectivity of the glycan biosensor constructed on a mixed SAM containing 16.7% of OEG-COOH was probed by analysis of two analytes (GOD-2C4 and DBA) and a non-specific binding probe (HSA). Moreover, a drift of the signal of the biosensor incubated only with PBS measured at the same time intervals as for GOD-2C4, HSA and DBA is shown, as well. For other assay conditions see legend to Fig. 1.

Europe PMC Funders Author Manuscripts

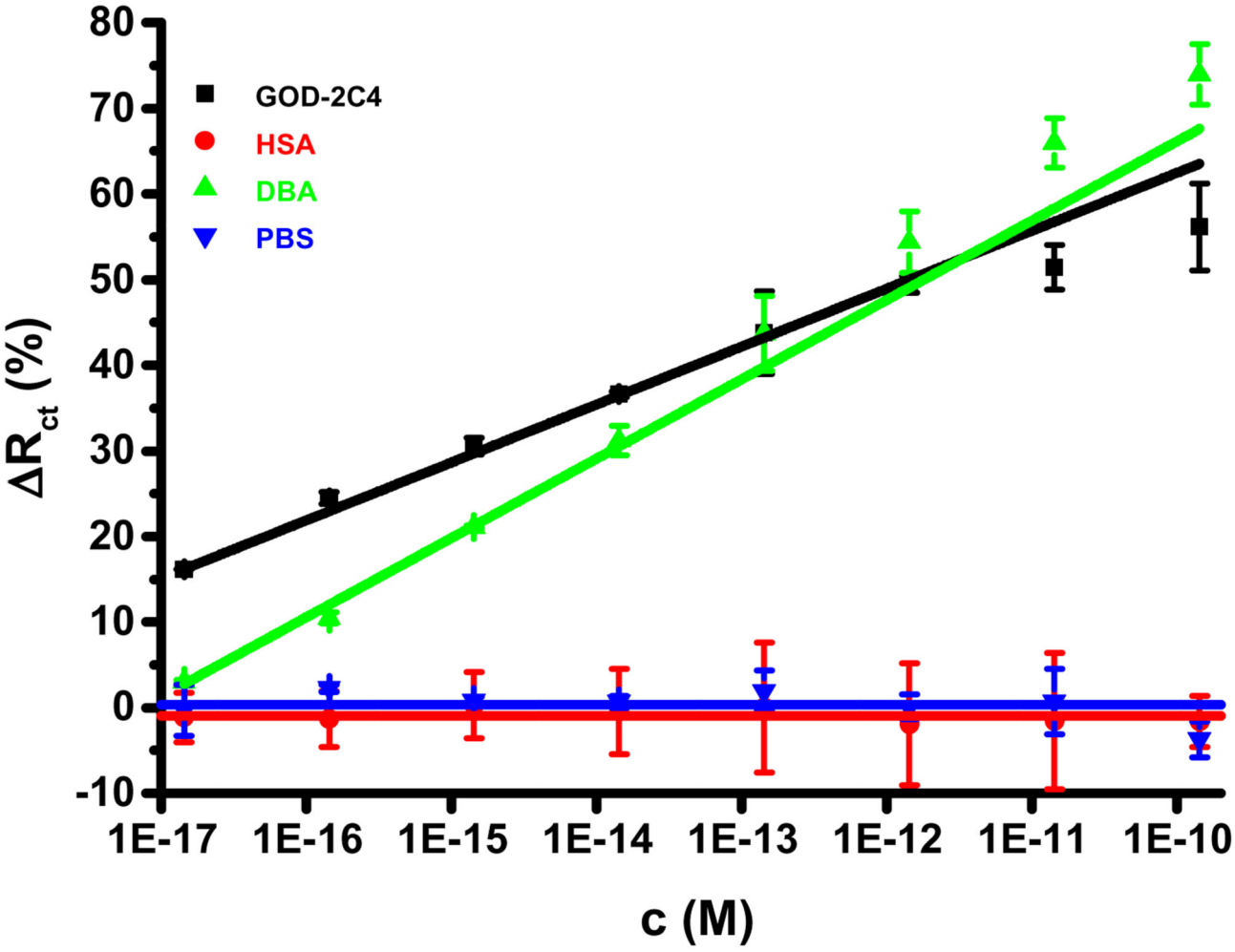

Figure 4.

Selectivity of the glycan biosensor constructed on HSA layer was probed by analysis of two analytes (GOD-2C4 and DBA) and a non-specific binding probe (HSA). Moreover, a drift of the signal of the biosensor incubated only with PBS measured at the same time intervals as for GOD-2C4, HSA and DBA is shown, as well. For other assay conditions see legend to Fig. 1.

Europe PMC Funders Author Manuscripts

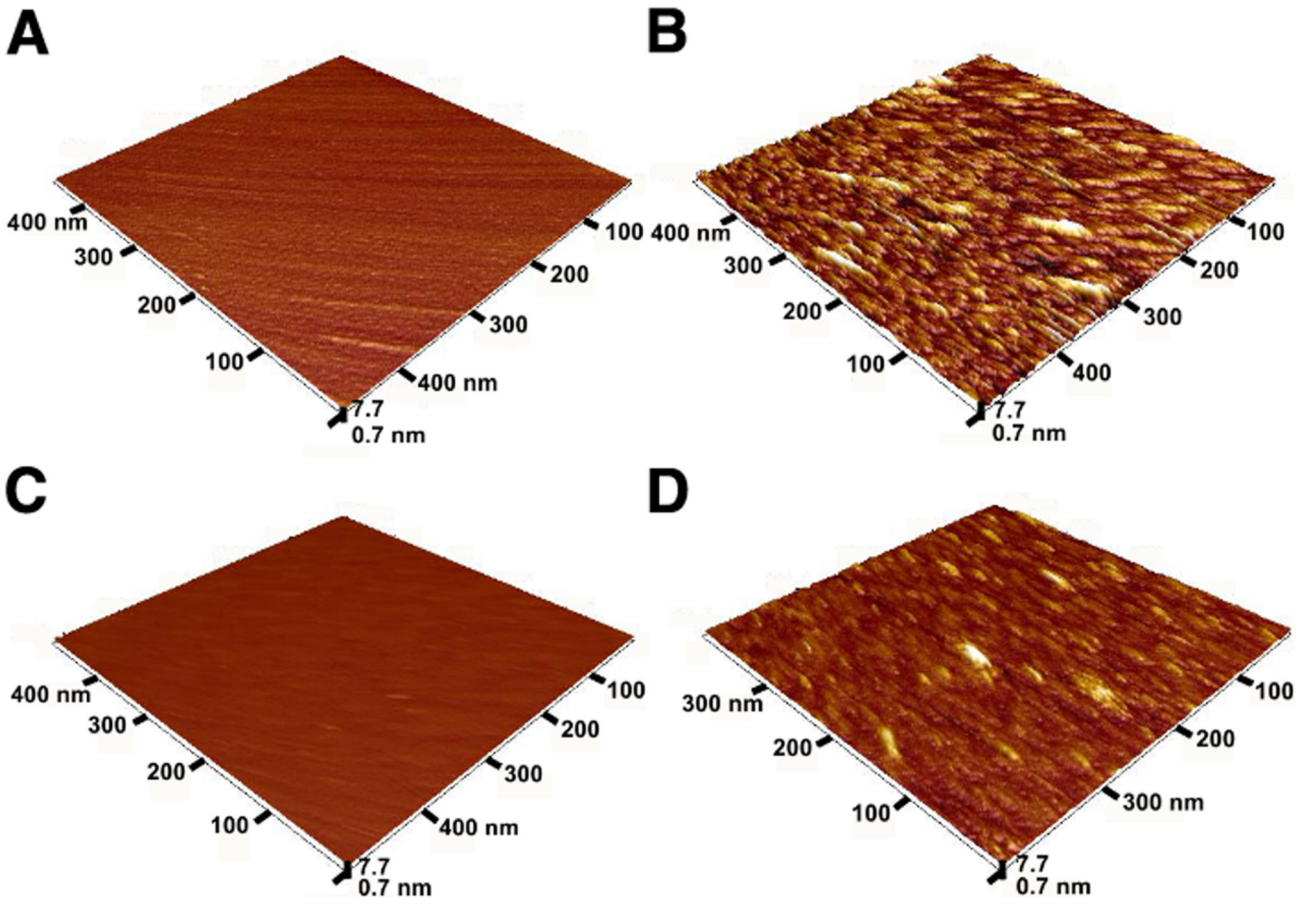

Figure 5.

AFM images of the glycan biosensor 2 before (**A**) and after incubation with GOD-2C4 analyte (**B**) and of the glycan biosensor 3 before (**C**) and after incubation with GOD-2C4 analyte (**D**). In all four AFM images z-axis is the same for better comparison of the size of features present on the surface.

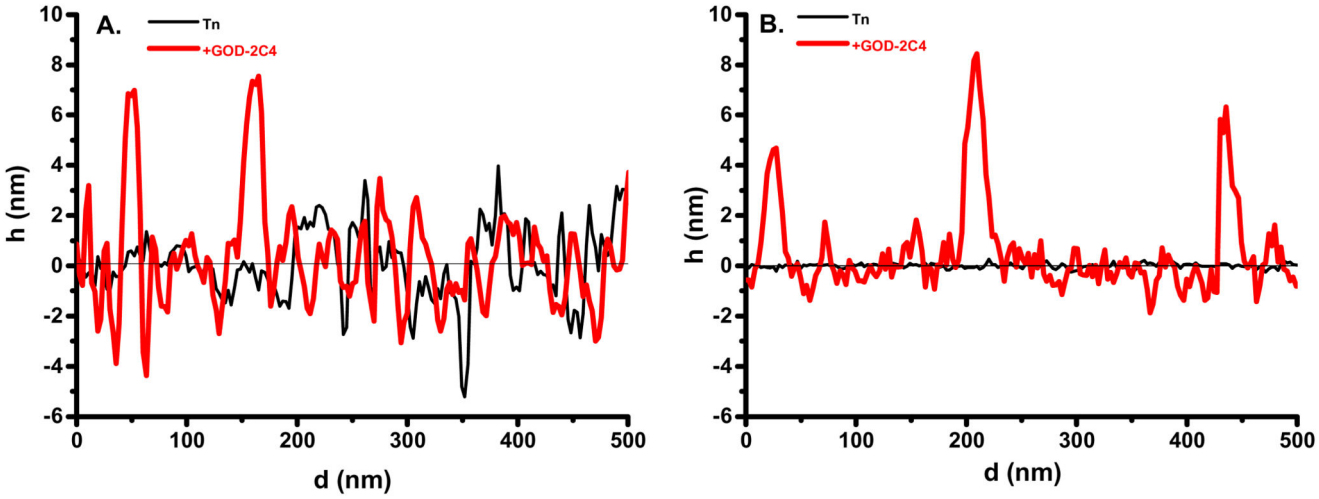

Figure 6.

AFM profile of the features present on the biosensor 2 interface before (Tn) and after incubation with GOD-2C4 analyte (+GOD-2C4) (**A**) and the features present on the biosensor 3 before and after interaction with GOD-2C4 analyte are shown, as well (**B**).

Europe PMC Funders Author Manuscripts